Neuroanatomical correlates of olfactory loss in normal aged subjects

Bàrbara Segura[1,2], Hugo Cesar Baggio[1,2], Elisabeth Solana[1,] Eva Palacios[1,2], Pere Vendrell [1,2], Nuria Bargallo[1,2] Carme Junqué[1,2,].

[1]Department of Psychiatry and Clinical Psychobiology, University of Barcelona. Barcelona. Spain

[2] Institute of Biomedical Research August Pi i Sunyer (IDIBAPS). Barcelona, Spain.

[3] Centre de Diagnòstic per la Imatge Hospital Clinic de Barcelona (CDIC), Hospital Clínic de Barcelona, Spain.

Corresponding author:

Prof. Carme Junque

Department of Psychiatry and Clinical Psychobiology. University of Barcelona

Casanova 143 (08036) Barcelona, Spain

Phone: (+34) 93 402 45 70 // Fax: (+34) 93 403 52 94 // E-mail: cjunque@ub.edu

Abstract

Postmortem studies have described that olfactory loss observed in normal aging is associated with Alzheimer's type brain degeneration. We hypothesized that distinct measures of gray and white matter integrity evaluated through magnetic resonance imaging (MRI) techniques could detect degenerative changes associated with age-related olfactory dysfunction. High-resolution T1-weighted images and diffusion-tensor images (DTI) of 30 clinically healthy subjects aged 51 to 77 were acquired with a 3-Tesla MRI scanner. Odor identification performance was assessed by means of the University of Pennsylvania Smell Identification Test (UPSIT). UPSIT scores correlated with right amygdalar volume and bilateral perirhinal and entorhinal cortices gray matter volume. Olfactory performance also correlated with postcentral gyrus cortical thickness and with fractional anisotropy and mean diffusivity levels in the splenium of the corpus callosum and the superior longitudinal fasciculi. Our results suggest that age-related olfactory loss is accompanied by diffuse degenerative changes that might correspond to the preclinical stages of neurodegenerative processes.

Key words: MRI; olfactory deficits; DTI; VBM; cortical thickness; UPSIT; aging.

INTRODUCTION

There is a large body of evidence linking olfactory loss and neurodegenerative processes. Olfactory impairments are strongly associated with Parkinson's (PD) and Alzheimer's (AD) diseases [1, 2], and have been investigated in animal models of AD [3].

In normal aging, the association between olfactory impairment and brain degeneration has been reported in a longitudinal clinicopathological study that included a large cohort of 471 elderly subjects (*Rush Memory and Aging Project*). During a mean follow-up of 2.2 years, autopsies were obtained from 122 of 166 subjects who died, revealing that scores in odor identification correlated with neuropathological changes usually associated with AD: density of neurofibrillary tangles in the entorhinal cortex and in the CA1 subfield of the hippocampus and the subiculum [4].

In a 5-year follow-up study including subjects from the same cohort, initial smell identification test scores were found to be associated with the risk of developing mild cognitive impairment (MCI). Moreover, in 34 subjects with olfactory dysfunction who died without cognitive deficits, autopsy showed greater burden of AD pathology [5].

The relationship between olfactory impairment and progressive cognitive decline was also seen in an epidemiological study involving 1,920 participants with a mean age of 66.9 years. In this study, authors reported an association between olfactory impairment and the incidence of MCI 5 years later with an odds-ratio of 6.62 [6].

Magnetic resonance imaging (MRI) is an invaluable tool for the study of "in vivo" brain correlates of olfactory dysfunctions. In PD, olfactory impairment has been found to be related to white matter integrity loss detected by MRI diffusion-tensor imaging

(DTI) [7]. On the other hand, voxel-based morphometry (VBM) studies have evidenced that subjects with hyposmia and anosmia of different etiology show gray and white matter reductions in central regions involved in the olfactory system [8, 9].

The purpose of the current study was to investigate the cerebral correlates of impairments in odor identification in a sample of clinically healthy subjects and to correlate the performance in odor identification with measures of MRI cerebral degeneration such as cortical thickness, gray matter volumes and measures of white matter integrity. We hypothesized that olfactory dysfunctions in older persons could be associated with brain olfactory regions but also with other brain regions sensitive to the preclinical stages of degenerative processes.

METHODS

Subjects.

The sample included 30 clinically healthy subjects (12 males; mean age: 66.0 $\pm$ 7.4 years, range, 51-77 years; mean years of education: 11.1 $\pm$ 4.2). All were right handed. All the participants were volunteers recruited from the Institut Català de l'Envelliment in Barcelona.

General exclusion criteria were: uncorrected visual or auditory deficits, drug abuse, and history of past or current psychiatric or neurologic disorder. Specific exclusion criteria for the olfaction test were: history of nasal bone fracture, diagnosis of rhinitis or nasal polyps, and upper respiratory tract infections in the 2 weeks prior to or at the moment of evaluation. Imaging exclusion criteria included any abnormality except mild white matter hyperintensities All selected participants completed a screening interview to check relevant medical information. One subject was currently a smoker, 7 had been smokers in the past and 22 had no history of smoking.

All subjects had normal general cognitive performance according to the Mini-Mental State Examination (scores ≥26) and normal global IQ scores (higher than 85) estimated by the Vocabulary subtest of the Wechsler Adult Intelligence Scale-III [12]. All participants underwent a comprehensive neuropsychological assessment.

The study was approved by the ethics committee of the University of Barcelona. All enrolled subjects signed an informed consent form before taking part in the study.

Olfactory assessment

Odor identification was assessed using the University of Pennsylvania Smell Identification Test (UPSIT) [13]. The UPSIT is a standardized forced-choice test comprised of four booklets containing 10 odorants apiece, 1 odorant per page. The stimuli are embedded in “scratch and sniff” microcapsules fixed and positioned on strips at the bottom of each page. A multiple-choice question with four response alternatives for each item is located above each odorant strip. Scores are calculated as the number of items correctly identified. Respondents can be placed into percentiles based on gender- and age-standardized norms for the number of correctly identified odorants. The UPSITs are packaged in envelopes and come with easy-to-follow instructions. Following normative data presented in the UPSIT manual, scores greater than 33 were considered to reflect normosmia and scores lower or equal to 18 were classified as anosmia. Scores between 19 and 32 reflected microsmia (from 19 to 25: severe microsmia; from 26 to 29: moderate microsmia and from 30 to 33: mild microsmia).

Neuropsychological assessment

We selected a neuropsychological battery including tests described as sensitive to aging effects and which have been found to be altered in the preclinical stages of Alzheimer's disease. The battery comprised tests measuring episodic memory (Rey Auditory Verbal Learning Test (RAVLT)), visuospatial and visuoperceptual functions (Benton's Judgment of Line Orientation and Facial recognition) and executive functions (Trail Making Test, Stroop Color-Word Test and 1 minute of phonetic (letters beginning with the letter P) and semantic (animals) fluencies). The characteristics of all tests are described in Lezak et al. (2004). Neuropsychological test results were analyzed using PASW-18 (Chicago, IL, http://www-01.ibm.com/software/analytics/spss/). Group differences in neuropsychological performance were tested using 3-level (normosmia, mild microsmia, moderate microsmia) one-way ANOVAs.

Image acquisition and analysis

Magnetic resonance images were acquired with a 3T scanner (MAGNETOM Trio, Siemens, Germany). High-resolution 3-dimensional T1-weighted images were acquired in the sagittal plane (TR 2300 ms, TE 2.98 ms, TI 900 ms; 256 x 256 matrix, 1 mm isotropic voxel). Sagittal diffusion tensor images were obtained using a single-shot EPI sequence (TR 5533 ms, TE 88 ms), with diffusion-encoding in 30 directions at b=0 and 1000 s/mm^2.

Structural data was analyzed with FSL-VBM [15], a voxel-based morphometry-style analysis carried out with FSL tools (http://fsl.fmrib.ox.ac.uk/fsl/fslwiki/FSL.) First, nonbrain tissue from structural images was extracted. After segmentation, GM images were aligned to MNI152 standard space using affine registration. The resulting images were averaged to create a study-specific template, to which the native GM images were then non-linearly re-registered. The registered partial volume images were then modulated (to correct for local expansion or contraction) by dividing by the Jacobian of

the warp field. The modulated segmented images were then smoothed with an isotropic Gaussian kernel with a sigma of 3 mm.

Voxelwise statistical analysis of fractional anisotropy (FA) and mean diffusivity (MD) data was carried out using TBSS (Tract-Based Spatial Statistics, [[16]]), part of FSL. First, FA and MD images were created by fitting a tensor model to the raw diffusion data using FDT, and then brain-extracted using BET [17]. All subjects' FA and MD data were then aligned into a common space using the nonlinear registration tool FNIRT (http://fsl.fmrib.ox.ac.uk/fsl/fslwiki/FNIRT) which uses a b-spline representation of the registration warp field [18]. Next, the mean FA and MD image were created and thinned to create a mean FA and MD skeleton which represents the centers of all tracts common to the group. Each subject's aligned FA and MD data were then projected onto this skeleton and the resulting data fed into voxelwise cross-subject statistics.

Structures used as regions of interest (ROIs) for GM analysis were chosen based on literature about the olfactory system. The included structures were the amygdala, hippocampus, parahippocampal gyrus (encompassing entorhinal and perirhinal areas), olfactory portion of the orbitofrontal cortex, gyrus rectus and insula bilaterally. The Automated Anatomical Labelling (AAL) atlas [19] was used to create the corresponding masks.

Finally, voxelwise general linear model was applied using permutation-based non-parametric testing (5000 permutations) for FA, MD and GM analyses, correcting for multiple comparisons across space using familywise error correction (FWE).

The estimation of cortical thickness was performed using the automated FreeSurfer stream (version 5.1; available at: http://surfer.nmr.harvard.edu). The procedures carried out by FreeSurfer software include removal of non-brain data, intensity normalization [20], tessellation of the gray matter/white matter boundary, automated topology correction [21, 22] and accurate surface deformation to identify tissue borders [23, 24, 25]). Cortical thickness is then calculated as the distance between the white and gray matter surfaces at each vertex of the reconstructed cortical

mantle [24]. Results for each subject were visually inspected to ensure accuracy of registration, skull stripping, segmentation, and cortical surface reconstruction.

The relationship between cortical thickness and UPSIT scores was assessed using a vertex-by-vertex general lineal model. Maps were smoothed using a circularly symmetric Gaussian kernel across the surface with a full width at half maximum (FWHM) of 15 mm. Z Monte Carlo simulations with 10,000 iterations were applied to CTh maps to provide cluster-wise correction for multiple comparisons, and results were thresholded at a corrected *p* value of 0.05 (Z = 1.3).

The automated procedure for volumetric measures of brain structures implemented in FreeSurfer was used to obtain the volumes of subcortical structures. Partial correlation between subcortical regions of interest (bilateral hippocampus and amygdala) and UPSIT scores, controlling for intracranial volume, were calculated using PASW-18 (Chicago, IL, http://www-01.ibm.com/software/analytics/spss/).

RESULTS

UPSIT scores ranged from 26 to 37 (mean 31.27, SD 2.95). Seven subjects (23.3%) were classified as normosmics; 15 (50%) had mild microsmia, 8 (26.7%) had moderate microsmia and none had severe microsmia or anosmia. There were no significant differences in these groups' neuropsychological test results (Table 1).

There were no significant correlations between age and UPSIT scores (r=-0.124 p=0.513). Additionally, UPSIT scores did not differ between males and females (t=0.09, p=0.920); thus, age and gender were not entered as covariates in the MRI models.

UPSIT scores correlated positively with cortical thickness in the right postcentral gyrus, indicating that olfactory dysfunction is associated with cortical thinning in this region (z=3.128; p<0.05, Montecarlo correction; cluster size: 1378.59 mm^2; x,y,z Talairach coordinates of the maximum: 48.3, -14.7, 42.3. (Figure 1)

Whole brain VBM analyses did not show any significant correlations at the corrected level. On the other hand, region-of-interest VBM analysis revealed a significant positive correlation between UPSIT scores and bilateral parahippocampal (entorhinal and perirhinal cortices) gray matter volumes. Left-side cluster: r=0.62; p=.017, FWE-correction; cluster volume: 776 mm^3; x,y,z MNI coordinates of the maximum: -26, -10, -34. Right-side cluster: r=0.63; p=.017, FWE-correction; cluster volume: 1296 mm^3; x,y,z MNI coordinates of the maximum: 20, -12, -28 (Figure 2). Moreover, UPSIT scores also correlated with the volume of the right amydgala corrected by intracranial volume (r=0.413, p=0.026)

Regarding DTI results, UPSIT scores correlated positively with FA and negatively with MD values in bilateral parietal as well as right temporal and right frontal white matter regions, corresponding to the topography of the superior longitudinal fasciculi, the inferior occipito-frontal fasciculus, anterior thalamic radiation, and the corpus callosum (Figure 3).

DISCUSSION

In this study, we found that olfactory loss in normal subjects correlated with several brain measures of gray and white matter integrity. We observed correlations of UPSIT scores with several structures involved in olfactory function such as the perirhinal and entorhinal cortices and the amygdala. Bitter et al. [8], using a VBM approach, described that subjects with anosmia of different etiology had gray matter reductions in primary as well as secondary olfactory regions. In the same line of our correlational data, they found gray matter volume reductions in anosmic patients in the parahippocampal gryrus, but they also found decrements in associative regions such as the medial prefrontal cortex. The widespread gray matter reductions they reported could be due to the fact that their subjects were anosmic (none of our subjects

presented anosmia) and that a more liberal threshold of significance (p<0.01, not corrected for multiple comparisons) was used. In their study, at the corrected level, only the medial/anterior cingulate region remained significant. The same group of research in a sample with less severe olfactory loss (hyposmic subjects) found gray matter reductions in the insular cortex, anterior cingulate cortex, orbitofrontal cortex, cerebellum, fusiform gyrus, precuneus, middle temporal gyrus and perirhinal cortex. However, the results were also obtained at an uncorrected level of significance. The authors interpreted their findings as secondary to the reduced olfactory input, because a subsample of subjects with hyposmia of peripheral origin of the olfactory impairment has similar gray matter reductions. The samples of both studies included young and old people thus aging effects could not be isolated.

In addition to the classical structures of the olfactory system, we also found correlations of UPSIT scores with cortical thickness in the neocortex. Specifically, we found that right postcentral gyrus thinning is related with poor performance in olfaction or in other words that thicker cortex in this region is associated with better performance in odor identification. Curiously, this result is in agreement with the data obtained by Frasnelli et al (2010) in a sample of 46 healthy young university students. These authors found that a composite olfactory score positively correlated with the performance and cortical thickness in the right dorsal postcentral gyrus. Thus, it is possible that such relationship in our sample reflected individual differences in odor perception acquired during young ages rather than aging effects.

DTI analyses have provided evidence of the association between degenerative brain changes and olfactory dysfunction in our sample. At the corrected level, we found that UPSIT scores positively correlated with FA scores and negatively with MD scores mainly involving the the corpus callosum and the superior longitudinal fasciculi. These results indicate that the loss of integrity of the cerebral fibers is related to loss of olfactory efficiency. The fibers that correlated with olfaction performance are not related

to the olfactory circuitry. In our opinion, this correlation reflects a common cause of degeneration for the olfactory system and other brain structures. Aging *per se* doesn't seem to be responsible for olfactory loss in our sample; we haven't observed any correlations between UPSIT scores and age. It is possible that a subsample of our subjects might instead be in the preclinical stage of a degenerative illness. This subsample could have both degeneration in limbic structures directly explaining the olfactory dysfunctions and subtle changes in the neocortical circuitry reflecting a more generalized degeneration.

There is wide evidence on the olfactory loss as a preclinical or prodromal sign of brain degeneration. Carriers of the CAG repeat expansion who are not yet diagnosed with Huntington's disease [26] have decreased UPSIT scores between 9 and 15 years before the estimated onset of the disease. Hyposmia is listed among the nonmotor symptom of PD (alongside constipation, daytime sleepiness, and rapid eye movement sleep behavior disorders and affective symptoms), and is also present in undiagnosed individuals at risk for PD (first-degree relatives of PD patients) [27], being considered a nonmotor feature which may precede by years the onset of motor disease [28-30]. Moreover, olfaction is impaired in PD patients with leucine-rich repeat kinase (*LRRK2*) G2019S mutations, and also in a subset of LRRK2 carriers without PD [31]. It has also been found that severe olfactory dysfunction is a prodromal symptom of dementia [32].

Hyposmia is seen in early stages of PD and in subjects with MCI [33, 34]. Higher density of entorhinal cortex and hippocampal neurofibrillary tangles correlates with greater deficits in odor identification, suggesting a role for hippocampal dysfunction in Alzheimer's disease hyposmia [4]. Olfactory dysfunctions are predictive of cognitive decline in the elderly and interact with the ApoEε4 allele [35-37]. Longitudinal MRI studies are needed to clarify the clinical significance of the specific brain changes associated with olfactory deficits in normal aging.

In summary, we found that olfactory loss in normal aged people is associated with impairment in some olfactory regions such as the amygdala, entorhinal and perirhinal cortex, but also with other cerebral regions not related with this function. The fact that individuals with olfactory loss had several signs of brain degeneration is in agreement with the idea that olfactory loss could be a preclinical marker of degenerative illness.

Acknowledgments

The authors would like to thank the Spanish Ministry of Science and Innovation for its funding to CJ, HCB and BS (PSI2010-16174) and the Generalitat de Catalunya for the funding of HCB (FI-DGR grant, 2011FI_B 00045), and support to the research Group neuropsychology (2009SGR-94)

Disclosure Statement:

All authors have contributed to the project and production of the manuscript and there is no conflict of interest.

References

[1] Mesholam RI, Moberg PJ, Mahr RN, Doty RL. Olfaction in neurodegenerative disease: a meta-analysis of olfactory functioning in Alzheimer's and Parkinson's diseases. Arch Neurol, 1998;55:84-90.

[2] Frasnelli J, Lundstrom JN, Boyle JA, Djordjevic J, Zatorre RJ, Jones-Gotman M. Neuroanatomical correlates of olfactory performance. Exp Brain Res, 2010;201:1-11.

[3] Wesson DW, Levy E, Nixon RA, Wilson DA. Olfactory dysfunction correlates with amyloid-beta burden in an Alzheimer's disease mouse model. J Neurosci, 2010;30:505-514.

[4] Wilson RS, Arnold SE, Schneider JA, Tang Y, Bennett DA. The relationship between cerebral Alzheimer's disease pathology and odour identification in old age. J Neurol Neurosurg Psychiatry, 2007;78:30-35.

[5] Wilson RS, Arnold SE, Schneider JA, Boyle PA, Buchman AS, Bennett DA. Olfactory impairment in presymptomatic Alzheimer's disease. Ann N Y Acad Sci, 2009;1170:730-735.

[6] Schubert CR, Carmichael LL, Murphy C, Klein BE, Klein R, Cruickshanks KJ. Olfaction and the 5-year incidence of cognitive impairment in an epidemiological study of older adults. J Am Geriatr Soc, 2008;56:1517-1521.

[7] Ibarretxe-Bilbao N, Junque C, Marti MJ, Valldeoriola F, Vendrell P, Bargallo N, Zarei M, Tolosa E. Olfactory impairment in Parkinson's disease and white matter abnormalities in central olfactory areas: A voxel-based diffusion tensor imaging study. Mov Disord, 2010;25:1888-1894.

[8] Bitter T, Bruderle J, Gudziol H, Burmeister HP, Gaser C, Guntinas-Lichius O. Gray and white matter reduction in hyposmic subjects--A voxel-based morphometry study. Brain Res, 2010;1347:42-47.

[9] Bitter T, Gudziol H, Burmeister HP, Mentzel HJ, Guntinas-Lichius O, Gaser C. Anosmia leads to a loss of gray matter in cortical brain areas. Chem Senses, 2010;35:407-415.

[10] Cummings JL, Mega M, Gray K, Rosenberg-Thompson S, Carusi DA, Gornbein J. The Neuropsychiatric Inventory: comprehensive assessment of psychopathology in dementia. Neurology, 1994;44:2308-2314.

[11] Beck, A.T., Steer, R.A,, Brown, G.K. Manual for the Beck Depression Inventory-II. San Antonio, 1996.

[12] Wechsler D. Wechsler Adult Intelligence Scale (WAIS III). Third ed. : Pearson, 1997.

[13] Doty RL. The Smell Identification Test. Administration Manual. Third ed. , 1995.

[14] Lezak, D.M, Howieson, D.B., Loring, D.W., Hannay, H.J., Fischer, J.S.,. Neuropsychological Assessment. Fourth ed. New York, 2004.

[15] Douaud G, Smith S, Jenkinson M, Behrens T, Johansen-Berg H, Vickers J, James S, Voets N, Watkins K, Matthews PM, James A. Anatomically related grey and white matter abnormalities in adolescent-onset schizophrenia. Brain, 2007;130:2375-2386.

[16] Smith SM, Jenkinson M, Johansen-Berg H, Rueckert D, Nichols TE, Mackay CE, Watkins KE, Ciccarelli O, Cader MZ, Matthews PM, Behrens TE. Tract-based spatial statistics: voxelwise analysis of multi-subject diffusion data. Neuroimage, 2006;31:1487-1505.

[17] Smith SM. Fast robust automated brain extraction. Hum Brain Mapp, 2002;17:143-155.

[18] Rueckert D, Sonoda LI, Hayes C, Hill DL, Leach MO, Hawkes DJ. Nonrigid registration using free-form deformations: application to breast MR images. IEEE Trans Med Imaging, 1999;18:712-721.

[19] Tzourio-Mazoyer N, Landeau B, Papathanassiou D, Crivello F, Etard O, Delcroix N, Mazoyer B, Joliot M. Automated anatomical labeling of activations in SPM using a macroscopic anatomical parcellation of the MNI MRI single-subject brain. Neuroimage, 2002;15:273-289.

[20] Sled JG, Zijdenbos AP, Evans AC. A nonparametric method for automatic correction of intensity nonuniformity in MRI data. IEEE Trans Med Imaging, 1998;17:87-97.

[21] Fischl B, Liu A, Dale AM. Automated manifold surgery: constructing geometrically accurate and topologically correct models of the human cerebral cortex. IEEE Trans Med Imaging, 2001;20:70-80.

[22] Segonne F, Pacheco J, Fischl B. Geometrically accurate topology-correction of cortical surfaces using nonseparating loops. IEEE Trans Med Imaging, 2007;26:518-529.

[23] Dale AM, Fischl B, Sereno MI. Cortical surface-based analysis. I. Segmentation and surface reconstruction. Neuroimage, 1999;9:179-194.

[24] Fischl B, Dale AM. Measuring the thickness of the human cerebral cortex from magnetic resonance images. Proc Natl Acad Sci U S A, 2000;97:11050-11055.

[25] Dale, A.M., Sereno, M.I. Improved localization of cortical activity by combining EEG and MEG with MRI cortical surface reconstruction: a linear approach. J Cogn Neurosci, 1993;5:162-176.

[26] Stout JC, Paulsen JS, Queller S, Solomon AC, Whitlock KB, Campbell JC, Carlozzi N, Duff K, Beglinger LJ, Langbehn DR, Johnson SA, Biglan KM, Aylward EH. Neurocognitive signs in prodromal Huntington disease. Neuropsychology, 2011;25:1-14.

[27] Siderowf A, Jennings D, Eberly S, Oakes D, Hawkins KA, Ascherio A, Stern MB, Marek K, PARS Investigators. Impaired olfaction and other prodromal features in the Parkinson At-Risk Syndrome Study. Mov Disord, 2012;27:406-412.

[28] Ponsen MM, Stoffers D, Booij J, van Eck-Smit BL, Wolters EC, Berendse HW. Idiopathic hyposmia as a preclinical sign of Parkinson's disease. Ann Neurol, 2004;56:173-181.

[29] Ponsen MM, Stoffers D, Twisk JW, Wolters EC, Berendse HW. Hyposmia and executive dysfunction as predictors of future Parkinson's disease: a prospective study. Mov Disord, 2009;24:1060-1065.

[30] Ross GW, Petrovitch H, Abbott RD, Tanner CM, Popper J, Masaki K, Launer L, White LR. Association of olfactory dysfunction with risk for future Parkinson's disease. Ann Neurol, 2008;63:167-173.

[31] Saunders-Pullman R, Stanley K, Wang C, San Luciano M, Shanker V, Hunt A, Severt L, Raymond D, Ozelius LJ, Lipton RB, Bressman SB. Olfactory dysfunction in LRRK2 G2019S mutation carriers. Neurology, 2011;77:319-324.

[32] Baba T, Kikuchi A, Hirayama K, Nishio Y, Hosokai Y, Kanno S, Hasegawa T, Sugeno N, Konno M, Suzuki K, Takahashi S, Fukuda H, Aoki M, Itoyama Y, Mori E,

Takeda A. Severe olfactory dysfunction is a prodromal symptom of dementia associated with Parkinson's disease: a 3 year longitudinal study. Brain, 2012;135:161-169.

[33] Christen-Zaech S, Kraftsik R, Pillevuit O, Kiraly M, Martins R, Khalili K, Miklossy J. Early olfactory involvement in Alzheimer's disease. Can J Neurol Sci, 2003;30:20-25.

[34] Djordjevic J, Jones-Gotman M, De Sousa K, Chertkow H. Olfaction in patients with mild cognitive impairment and Alzheimer's disease. Neurobiol Aging, 2008;29:693-706.

[35] Wang QS, Tian L, Huang YL, Qin S, He LQ, Zhou JN. Olfactory identification and apolipoprotein E epsilon 4 allele in mild cognitive impairment. Brain Res, 2002;951:77-81.

[36] Wilson RS, Schneider JA, Arnold SE, Tang Y, Boyle PA, Bennett DA. Olfactory identification and incidence of mild cognitive impairment in older age. Arch Gen Psychiatry, 2007;64:802-808.

[37] Olofsson JK, Nordin S, Wiens S, Hedner M, Nilsson LG, Larsson M. Odor identification impairment in carriers of ApoE-varepsilon4 is independent of clinical dementia. Neurobiol Aging, 2010;31:567-577.

Table

Neuropsychological tests	Normosmics (n=7)	Mild hiposmics (n=15)	Moderate hiposmics (n=8)	F/*p*
MMSE	29.3 ± 1.1	29.8 ± 0.4	29.5 ± 0.5	1.565 / 0.227
Memory				
RAVLT learning	44.7 ± 5.2	44.5 ± 6.0	43.6 ± 4.3	0.096 / 0.909
RAVLT delayed recall	8.4 ± 2.1	8.9 ± 2.0	9.6 ± 2.1	0.697 / 0.507
RAVLT recognition	13.3 ± 2.1	13.7 ± 1.4	14.0 ± 1.1	0.423 / 0.659
Executive Functions				
TMT A, *seconds*	35.3 ± 14.6	39.3 ± 13.2	41.6 ± 13.2	0.419 / 0.662
TMT B, *seconds*	92.3 ± 51.7	90.0 ± 33.3	107.3 ± 26.0	0.605 / 0.553
SCWT, words	101.7 ± 20.8	96.3 ± 16.0	100.8 ± 7.3	0.386 / 0.683
SCWT, color	63.6 ± 11.5	59.6 ± 17.9	62.5 ± 12.0	0.195 / 0.824
SCWT, interference	6.6 ± 6.3	2.9 ± 7.9	-2.3 ± 7.4	0.996 / 0.382
Digits - forward span	5.8 ± 1.6	5.5 ± 1.5	5.5 ± 1.2	0.116 / 0.891
Digits - backward span	4.5 ± 1.6	4.2 ± 1.1	3.4 ± 0.9	1.886 / 0.172
Phonemic verbal fluency	16.0 ± 4.7	16.7 ± 5.9	17.3 ± 5.5	0.095 / 0.910
Semantic verbal fluency	20.0 ± 2.9	20.7 ± 4.6	23.3 ± 8.2	0.766 / 0.475
Visuospatial and visuoperceptual				
JLO	24.4 ± 6.7	23.0 ± 4.4	22.9 ± 2.9	0.263 / 0.771
Facial recognition	44.6 ± 3.6	46.7 ± 3.4	43.5 ± 3.7	2.405 / 0.109

Table 1. Neuropsychological assessment results in mean ± standard deviation.F/*p*: F-test and significance level of one-way ANOVAs comparing the 3 groups. MMSE: Mini-Mental State Examination, RAVLT: Rey Auditory Verbal Learning Test, TMT: Trail Making test, SCWT: Stroop Color-Word Test, JLO: Benton's Judgment of Line Orientation Test

Figure legends

Figure 1. Area of signiticant (p<0.05, Monte Carlo-corrected) positive correlation between UPSIT scores and right postcental gyrus cortical thickness.

Figure 2. VBM results: areas of significant (p<0.05, FWE-corrected) positive correlation between UPSIT scores and perirrhinal and enthorrinal cortex GM volume.

Figure 3. DTI results. Areas of significant (p<0.05, FWE-corrected) correlations between UPSIT and FA (red) and MD (blue) values. Plots represent the positive (FA) and negative (MD) correlations.

Figure 1

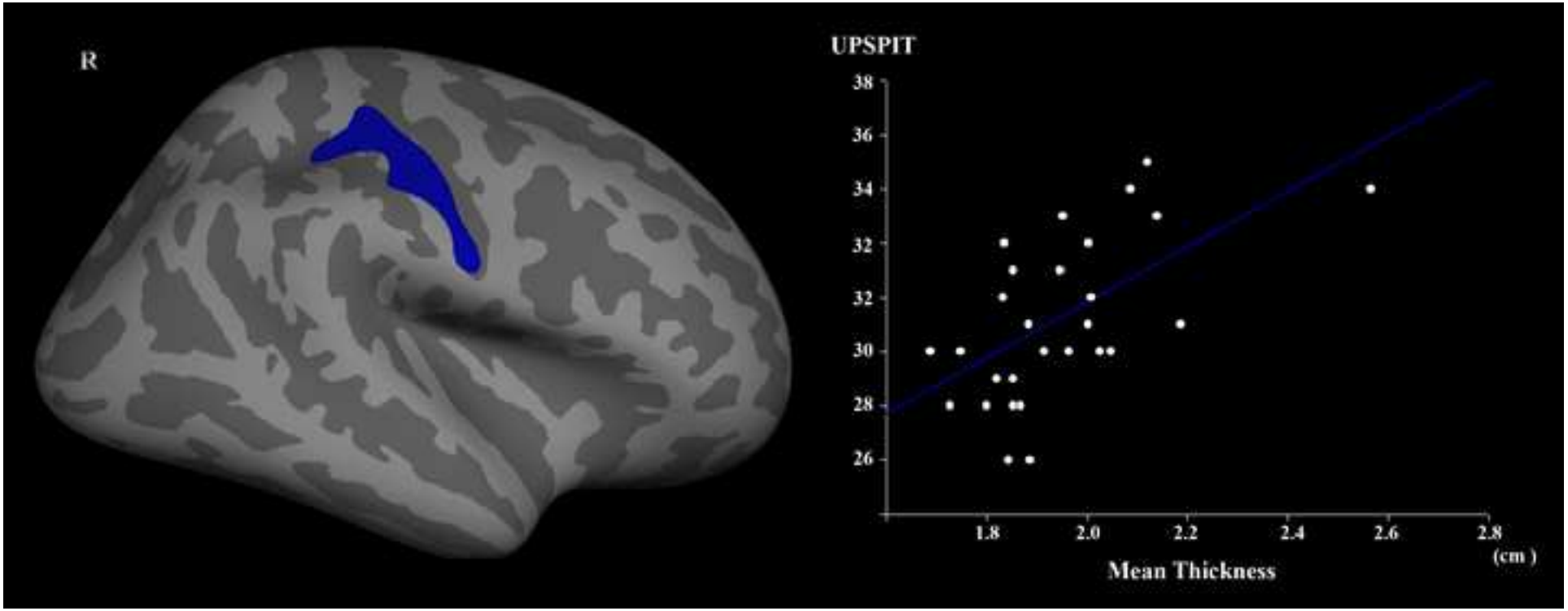
R
UPSPIT
38
36
34
32
32
30
28
26
1.8
2.0
2.2
2.4
2.6
2.8
(cm)
Mean Thickness

Figure 2

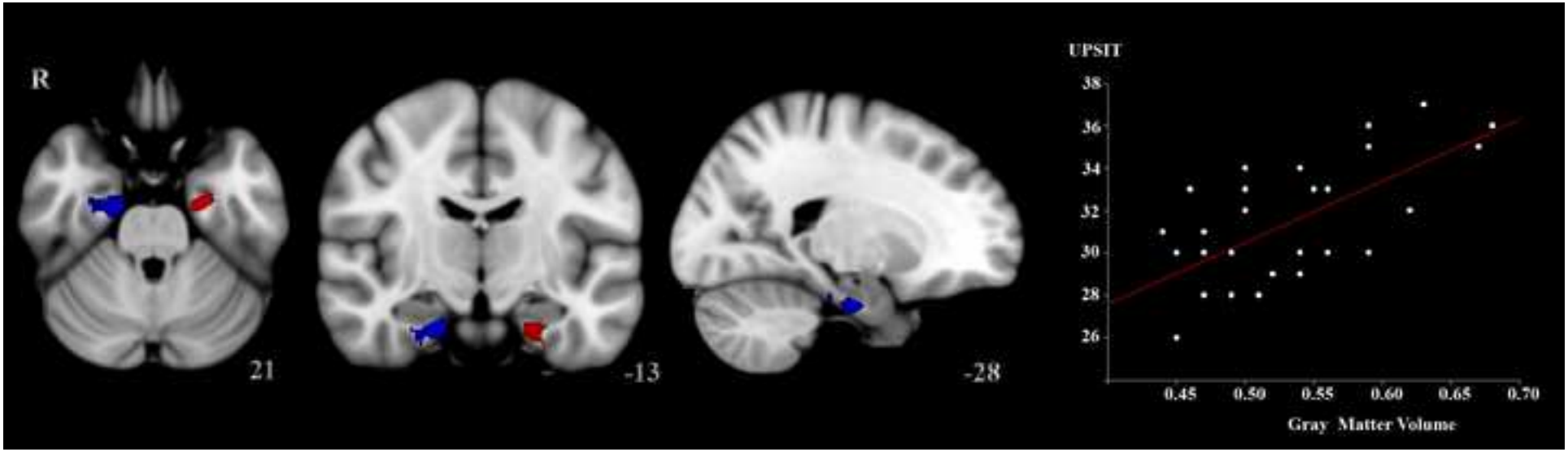
R
21
-13
-28
UPSIT
38
36
34
32
30
28
26
0.45
0.50
0.55
0.60
0.65
0.70
Gray Matter Volume

Figure 3

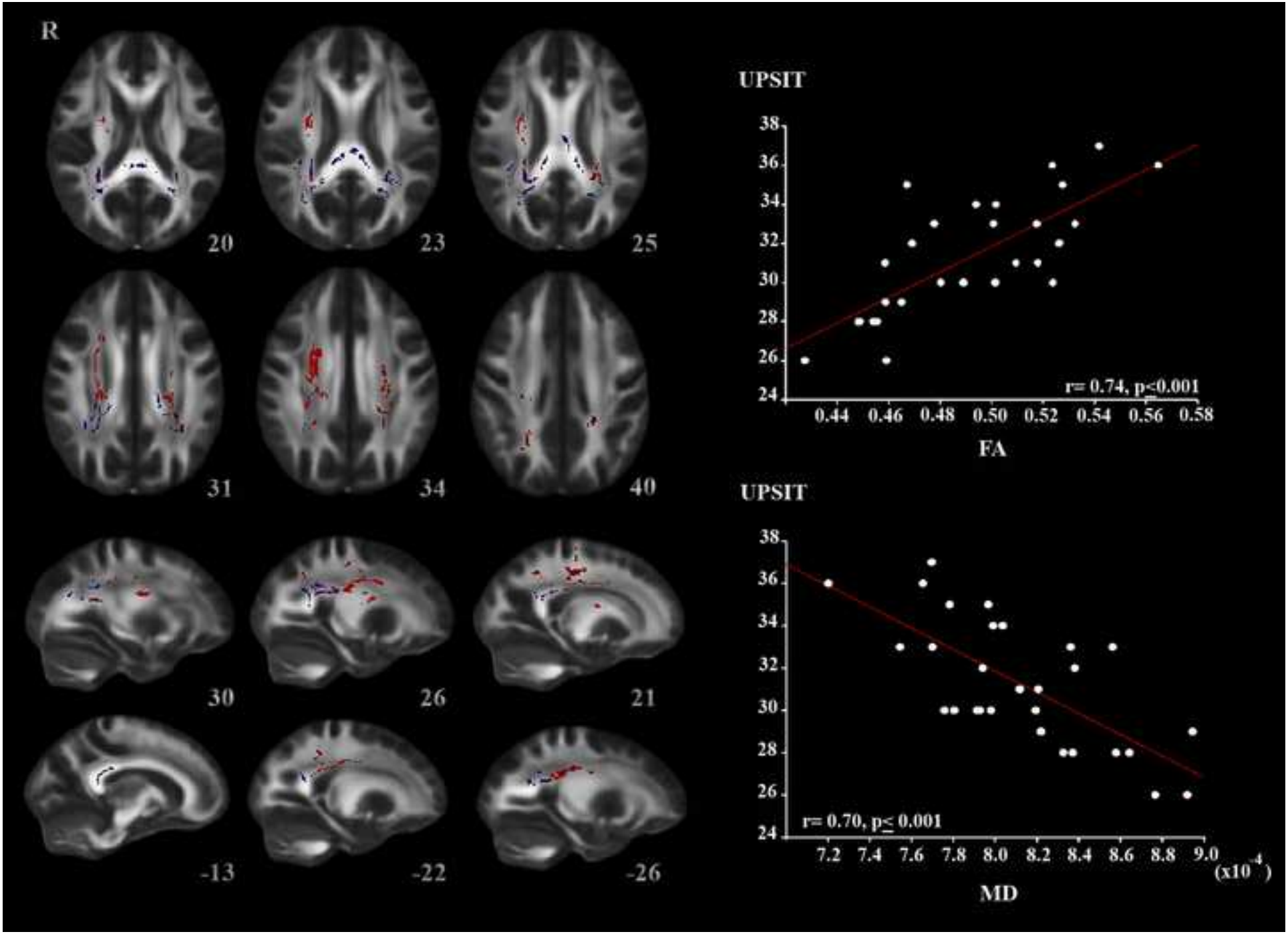
R
20
23
25
31
34
40
30
26
21
-13
-22
-26
UPSIT
38
36
34
32
30
28
26
24
r= 0.74, p<0.001
0.44 0.46 0.48 0.50 0.52 0.54 0.56 0.58
FA
UPSIT
38
36
34
32
30
28
26
24
r= 0.70, p≤ 0.001
7.2 7.4 7.6 7.8 8.0 8.2 8.4 8.6 8.8 9.0
(x10 -4)
MD